Research Paper

Exploring the molecular mechanism of glycyrrhetinic acid in the treatment of gastric cancer based on network pharmacology and experimental validation

Xia Li[1], Yuhua Du[1], Shicong Huang[1], Yi Yang[2], Doudou Lu[4], Junfei Zhang[4], Yan Chen[3], Lei Zhang[5], Yi Nan[3,5], Ling Yuan[1]

[1]College of Pharmacy, Ningxia Medical University, Yinchuan 750004, Ningxia Hui Autonomous Region, China
[2]College of Basic Medicine, Ningxia Medical University, Yinchuan 750004, Ningxia Hui Autonomous Region, China
[3]Traditional Chinese Medicine College, Ningxia Medical University, Yinchuan 750004, Ningxia Hui Autonomous Region, China
[4]College of Clinical Medicine, Ningxia Medical University, Yinchuan 750004, Ningxia Hui Autonomous Region, China
[5]Key Laboratory of Hui Ethnic Medicine Modernization of Ministry of Education, Ningxia Medical University, Yinchuan 750004, Ningxia Hui Autonomous Region, China

Correspondence to: Yi Nan, Ling Yuan; **email:** 20080011@nxmu.edu.cn, 20080017@nxmu.edu.cn
Keywords: glycyrrhetinic acid, gastric cancer, network pharmacology, molecular docking, MAPK signaling pathway
Received: February 13, 2023 **Accepted:** April 25, 2023 **Published:** May 11, 2023

ABSTRACT

There is a wide range of pharmacological effects for glycyrrhetinic acid (GRA). Previous studies have shown that GRA could inhibit the proliferation of tumor cells, showing a promising value in the treatment of gastric cancer (GC). Nonetheless, the precise mechanism of the effect of GRA on GC remains unclear. We explored cellular and molecular mechanisms of GRA based on network pharmacology and *in vitro* experimental validation. In this study, we predicted 156 potential therapeutic targets for GC with GRA from public databases. We then screened the hub targets using protein-protein interaction network (PPI) and conducted clinical correlation analysis. Gene Ontology (GO) enrichment and Kyoto Encyclopedia of Genes and Genomes (KEGG) pathway enrichment showed that GRA made anti-GC effects through multiple targets and pathways, particularly the MAPK signaling pathway. Next, molecular docking results revealed a potential interaction between GRA and MAPK3. In addition, qRT-PCR experiments revealed that 18β-GRA was able to suppress mRNA expression of *KRAS*, *ERK1* and *ERK2* in AGS cells. Western blotting results also revealed that 18β-GRA was able to suppress the expression of KRAS and p-ERK1/2 proteins in AGS cells. Additionally, immunofluorescence assays revealed that 18β-GRA inhibited p-ERK1/2 nuclear translocation in AGS cells. These results systematically reveal that 18β-GRA may have anti-tumor effects on GC by modulating the MAPK signaling pathway.

INTRODUCTION

Gastric cancer (GC) is a familiar digestive tract malignancy, ranking fifth for incidence and third for mortality worldwide [1]. GC can be caused by environmental factors, diet, Helicobacter pylori infection, and individual factors [2]. In addition, the occurrence of GC has been linked to gender, family history, history of gastric disease, and occupation. The main treatments for GC are drug therapy, chemotherapy, and surgery, however, they all have poor therapeutic results [3]. In the early phase, GC has inconspicuous clinical symptoms, so once it is detected, it is generally at a moderate to advanced stage and

accompanied by metastasis, which makes detection and treatment even more challenging with its high incidence and insidious features. Unfortunately, the prognosis for current treatments for GC is typically poor [4, 5]. Thus, it is pretty significant to find effective drugs which can cure GC.

Licorice is an extremely famous traditional Chinese medicine (TCM) that is commonly used in clinics. It is made from dried licorice roots and rhizomes and is available in the form of decoction pieces. Apart from its pharmacological value, licorice is also widely used in various foods for its nutritional and flavoring properties. Modern research has identified flavonoids, triterpenes, and polysaccharides as the main biologically active compounds in licorice [6, 7]. Glycyrrhetinic acid (GRA), an oleanane-type pentacyclic triterpenoid compound, is one of the major active components of licorice. GRA has multiple pharmacological effects, including anti-inflammatory, anti-tumor, antiviral, immuno-modulatory, and similar [8–11]. GRA has two optical isomers, 18α-GRA and 18β-GRA. Their structures are shown below (Figure 1). 18β-GRA has a stronger antitumor effect than 18αGRA, and it has been found that 18β-GRA has a significant inhibitory effect in multiple types of tumors, such as breast cancer [12], hepatocellular cancer [13], lung cancer [14], ovarian cancer [15], and gastric cancer [16]. The main mechanisms of 18β-GRA can not only inhibit tumor cell proliferation, and promote tumor cell apoptosis, but also inhibit tumor cell invasion and migration. Of course, it also can inhibit tumor angiogenesis [17]. Previous studies have demonstrated that 18β-GRA can improve the inflammatory microenvironment by downregulating COX-2 and upregulating miR-149-3p to inhibit Wnt-1, thereby inhibiting the occurrence and progression of GC [18]. In addition, some studies have reported that 18β-GRA can inhibit the invasion and migration of GC cells through the ROS/PKC-α/ERK pathway [19]. Recently, it was found that 18β-GRA can regulate the apoptosis signaling pathway associated with MRPL35, and inhibit GC cells proliferation [20].

Network pharmacology is an essential component of bioinformatics, which combines bioinformatics with systems medicine. Network pharmacology embodies the multi-component, multi-functional, and multi-faceted characteristics of TCM. Recently, people have used it to research TCM [21–23]. We predicted the potential mechanism for GRA in GC treatment through network pharmacology, designed experiments to test these predictions, and proposed different directions and ideas for future research. This study workflow is illustrated in Figure 2.

RESULTS

Common targets mining

We used network pharmacology to predict GRA's potential mechanism in the GC therapy and obtained 160 GRA and 15274 GC relevant targets with the target prediction website (Figure 3A). Afterwards, we made a Venn diagram for the GRA and GC targets, and screened 156 common targets (Figure 3B).

Constructing the PPI network and analysing hub targets

To further explore the relationship between 156 common targets, we analyzed the common targets through the STRING website (Figure 3C) and obtained the PPI network. We analyzed the PPI network using Cytoscape 3.8.2 (Figure 3D). On the basis of degree value analysis, the top 10 hub targets in the PPI network are TNF (degree = 53), IL-6 (degree = 52), CTNNB1 (degree = 42), PPARG (degree = 39), PTGS2 (degree = 38), ESR1 (degree = 37), MAPK3 (degree = 31), PPARA (degree = 28), AR (degree = 25), and CYP19A1 (degree = 25)

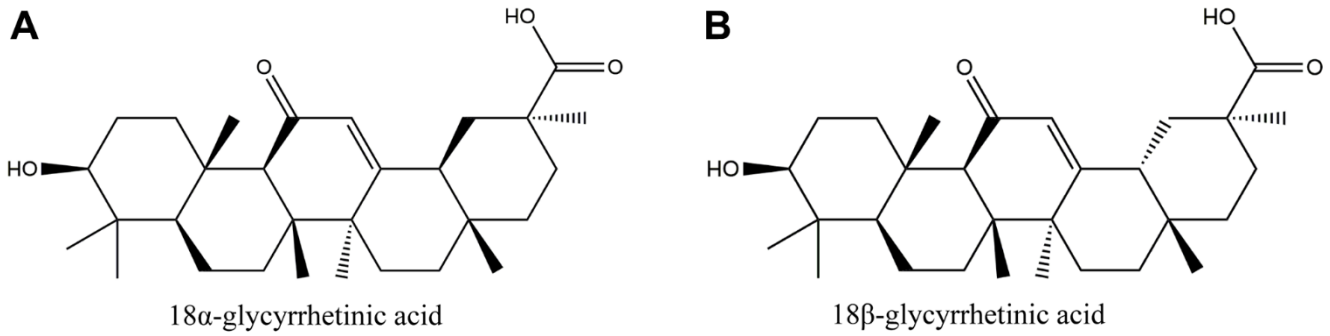

Figure 1. The structure of glycyrrhetinic acid (GRA). (**A**) 18α-glycyrrhetic acid (18α-GRA). (**B**) 18β-glycyrrhetic acid (18β-GRA).

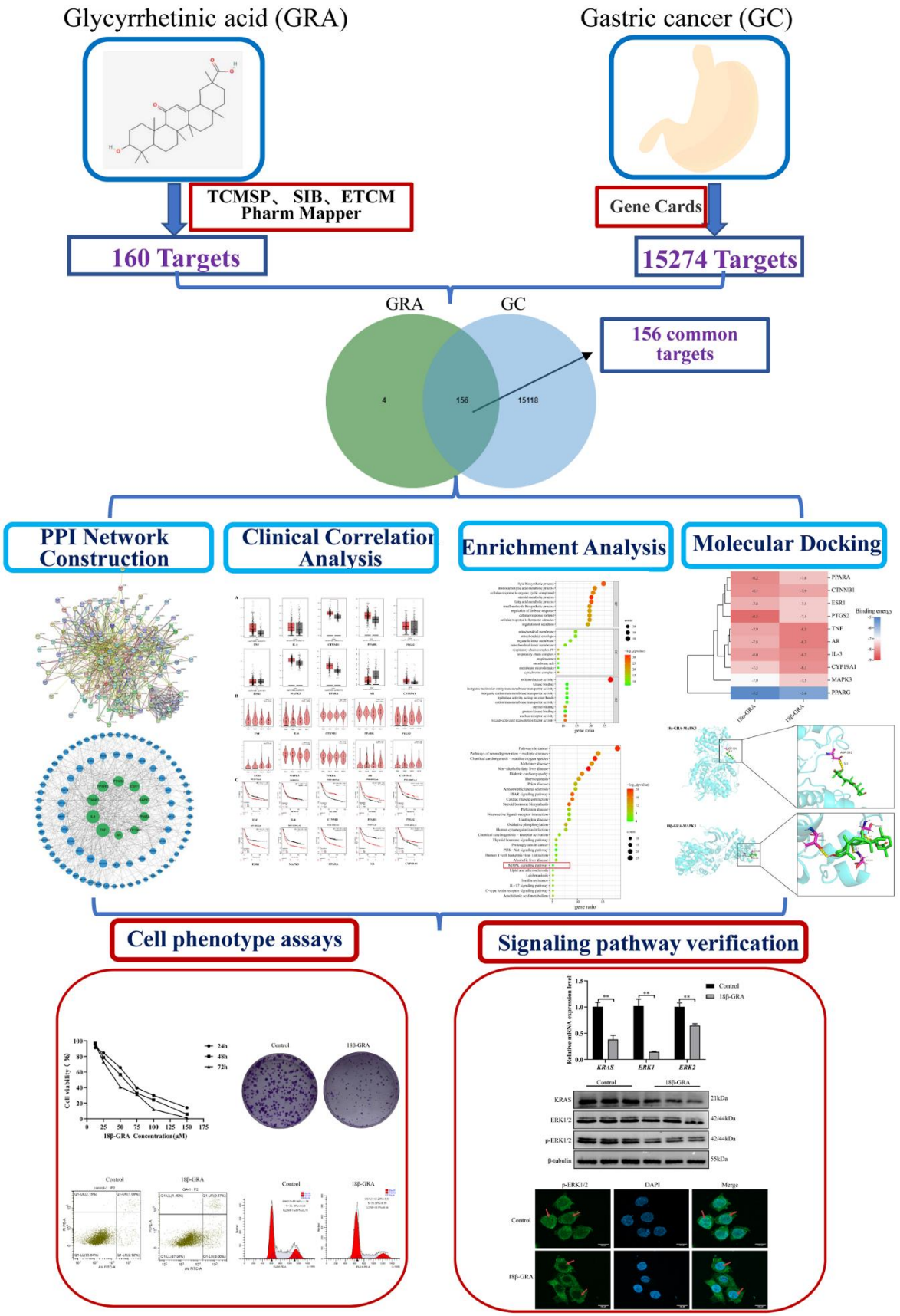

Figure 2. Workflow of the present study in a graphical manner.

(Figure 3E). The common target's degree value were shown in Supplementary Table 1. DEGs were analyzed by the GEO database. We used |log2(fold change)| > 1 and $p < 0.05$ in the volcano diagram, with red representing upregulated genes and green representing downregulated genes. *PPARG* (p = 0.00333) obviously downregulated, meanwhile *PTGS2* (p = 0.0144) and *CYP19A1* (p = 0.00664) obviously upregulated (Figure 3F).

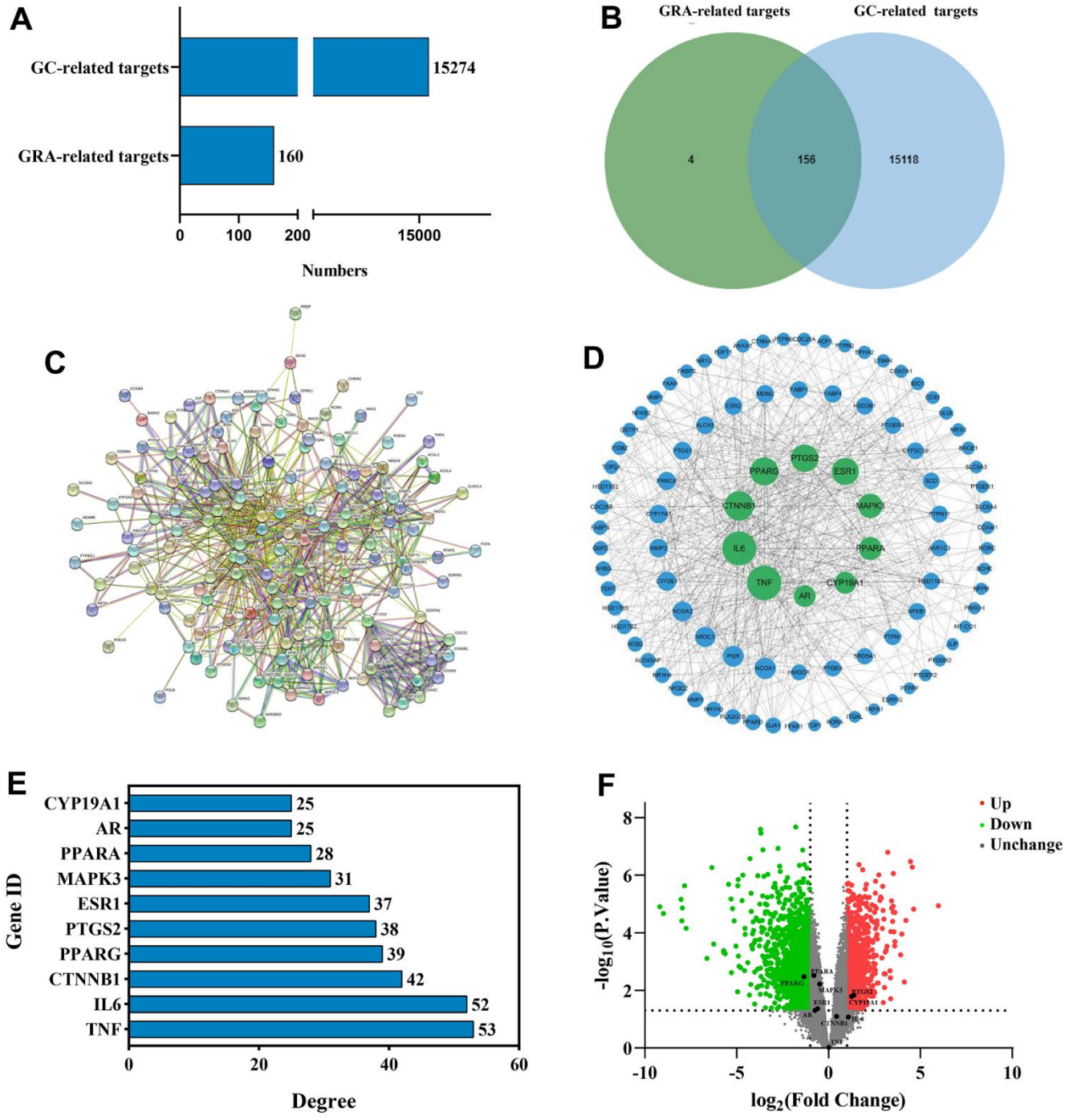

Figure 3. Identification of common targets and analysis of PPI network. (**A**) Potential targets of GRA-related and GC-related. (**B**) Venn diagram was applied to obtain the common targets between the GC targets and GRA targets. (**C**) PPI network of 156 common targets constructed with STRING. (**D**) The hub targets of PPI network. Larger node sizes indicate higher degree, green indicates higher degree, and blue indicates lower degree. (**E**) The PPI network's 10 hub targets ranked by degree ≥ 25. (**F**) Volcano plot of differentially expressed genes in GC. Red represents upregulated genes and green represents downregulated genes.

When we compared the normal group to the GC group in GEPIA, we discovered that *CTNNB1* mRNA expression was upregulated (Figure 4A). *TNF* (p = 0.0284), *PPARG* (p = 0.0379) and *ESR1* (p = 0.0268) were significant in tumor staging in GC patients (Figure 4B). We found that patients who had higher expression of *TNF* (p = 0.00039), *ESR1* (p = 1.1E-06), *MAPK3* (p =1.2E-07), *PPARA* (p = 3.9E-06) and AR(p =6.7E-11) had worse survival than patients who had lower expression, while the opposite was true for *CTNNB1* (p = 7E-08), *PTGS2* (p = 0.0083), *PPRAG* (p = 0.00022) and *CYP19A1* (p = 0.013), in the Kaplan-Meier plotter database (Figure 4C). When the $p < 0.001$ was reached, we considered the gene to be a prognostic marker for GC (Criteria for prognostic markers were reference to The Human Protein Atlas website). Based on the p value, *TNF*, *CTNNB1*, *PPARG*, *ESR1*, *MAPK3*, *PPARA* and *AR* can be used as prognostic markers of GC.

GO and KEGG enrichment analysis

We performed it to further explore the potential mechanisms of GRA treatment of GC, The top 10 enrichment terms of biological processes (BP), cellular components (CC), and molecular function (MF) were presented in a bubble diagram (Figure 5A). The results of GO enrichment analysis suggested that common targets were mainly related to BP and metabolic process, such as lipid biosynthetic process, mono-carboxylic acid metabolic process, steroid metabolic process, fatty acid metabolic process, and small molecule biosynthetic process. The MF mainly involved enzyme activity, transmembrane transporter activity, and receptor activity. Additionally, the CC were primarily associated with protein complexes and mitochondria. We also performed KEGG pathway enrichment analysis for common targets and the results showed that GRA modulates GC progression through multiple pathways associated with survival, differentiation, division and apoptosis (Figure 5B). Among them, MAPK signaling pathway is often activated in tumors, and its related proteins' abnormal expression and tumors' occurrence go hand in hand (Figure 5C).

Molecular docking

Molecular docking verifies the binding energy of GRA and hub targets. The results of 18α-GRA and 18β-GRA docking with hub targets (Figure 6A). A binding energy < -5.0 kcal/mol indicates excellent binding capability. The results showed that GRA can be combined with all the hub targets (Figure 6B). 18α-GRA and MAPK3 binding energy was -7.0 kcal/mol (Figure 6C), and 18β-GRA to MAPK3 was -7.5 kcal/mol (Figure 6D).

18β-GRA inhibited the GC cells proliferation

Consequently, we designed experiments to validate our prediction. 18β-GRA's effect on AGS cells viability was demonstrated by the CCK-8 method. We treated AGS cells with different concentrations of 18β-GRA for 24 h, 48 h, and 72 h for cell viability assay. The results demonstrated that 18β-GRA could significantly decrease AGS cells viability in a dose-dependent manner (Figure 7A). The IC_{50} of 18β-GRA intervention on AGS cells is shown in Figure 7B. The IC_{50} of AGS cells treated with 18β-GRA for 24 h was 63.56 μM, so 63.56 μM intervention for 24 h was the dose administered in our subsequent experiments. As shown in Figure 7C, 7D, 18β-GRA effect on AGS cells colony formation ability was observed. The results showed that the cell colony formation ability of 18β-GRA intervention group was obviously lower ($p < 0.001$) compared with the control group.

18β-GRA promoted GC cells apoptosis and arrested cell cycle

To further explore the ability of 18β-GRA to inhibit AGS cells proliferation, we analyzed the cells cycle in AGS and apoptosis with 18β-GRA intervention in AGS cells. Flow cytometry function was to confirm the effect of 18β-GRA on AGS cells apoptosis. The results illustrated that 18β-GRA made AGS cells apoptotic rate increase from 3.64 ± 0.50% to 10.67 ± 0.31% ($p < 0.001$) (Figure 7E, 7F). 18β-GRA effect on cell cycle distribution was detected. The results suggested that the G0/G1 proportion increased in the 18β-GRA intervention group (Figure 7G, 7H). The G0/G1 proportion was 63.20 ± 0.55%, which was higher than the control group's 44.64 ± 5.18% ($p < 0.001$). The above results indicated that 18β-GRA can effectively promote AGS cells apoptosis, arrest the AGS cell cycle in the G0/G1 phase, and thus have certain effects on AGS cells proliferation.

18β-GRA inhibited the related targets expression of MAPK signaling pathway

To identify the expression of hub targets in the MAPK signaling pathway, we used western blotting, qRT-PCR, and immunofluorescence techniques. The results of the qRT-PCR experiment demonstrated that the mRNA expression levels of *KRAS* ($p < 0.01$), *ERK1* ($p < 0.01$) and *ERK2* ($p < 0.01$) obviously decreased in 18β-GRA intervention group (Figure 8A). According to the results of western blotting, KRAS ($p < 0.01$) and p-ERK1/2 ($p < 0.01$) decreased in the 18β-GRA intervention group, and ERK1/2 did not alter significantly ($p > 0.05$) (Figure 8B, 8C).

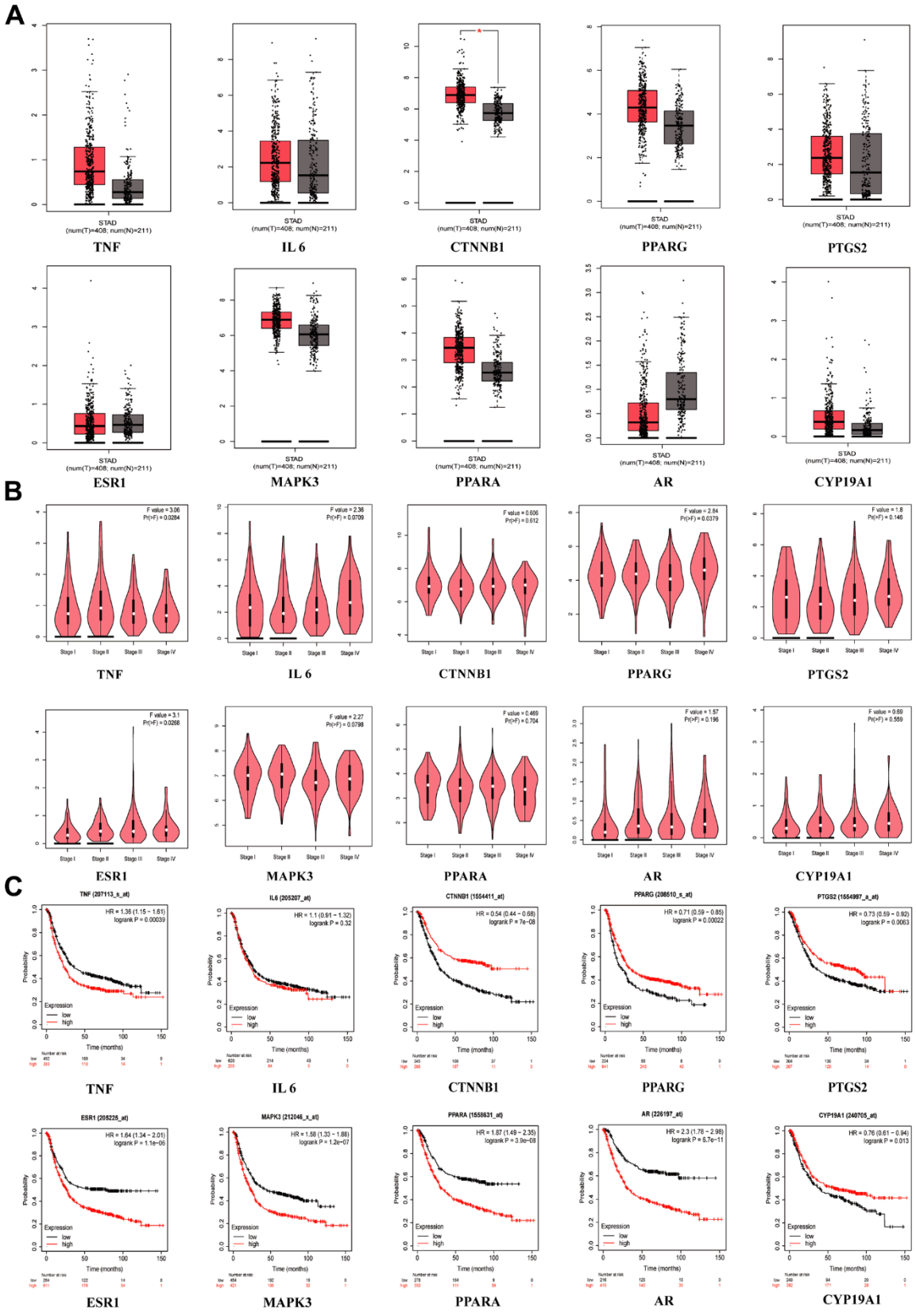

Figure 4. Clinical correlation analysis of hub targets. (**A**) mRNA expression level of hub targets between GC tissues and normal gastric tissues, **p* <0.05. (**B**) The significance of hub target in staging of GC, *p* <0.05 is considered to be statistically significant. (**C**) Survival analysis of hub targets, Log-rank *p* <0.05 is considered to be statistically significant.

An immunofluorescence assay was employed to find the nuclear translocation of p-ERK1/2 brought on by 18β-GRA intervention. The results demonstrated that the p-ERK1/2 expression in the cell nucleus decreased in the 18β-GRA intervention group ($p < 0.001$) (Figure 8D, 8E).

DISCUSSION

For thousands of years, the Chinese have used natural herbs in clinical settings. Nowadays, it has been attracting increasing attention due to its wide range of pharmacological effects. Numerous studies have shown that some herbal extracts and monomeric components have an essential anticancer role [24]. TCM has multiple targets, pathways, and mechanisms of action [25], but it is challenging to clarify them. Recently, the combination of bioinformatics analysis and pharmacology has been complemented by network pharmacology. People use it to systematically elucidate the mechanisms of TCM.

This study utilized public databases to predict the relationship between GRA and GC, and analyzed the PPI network to identify hub targets. The key target MAPK3 in the MAPK signaling pathway ranks higher

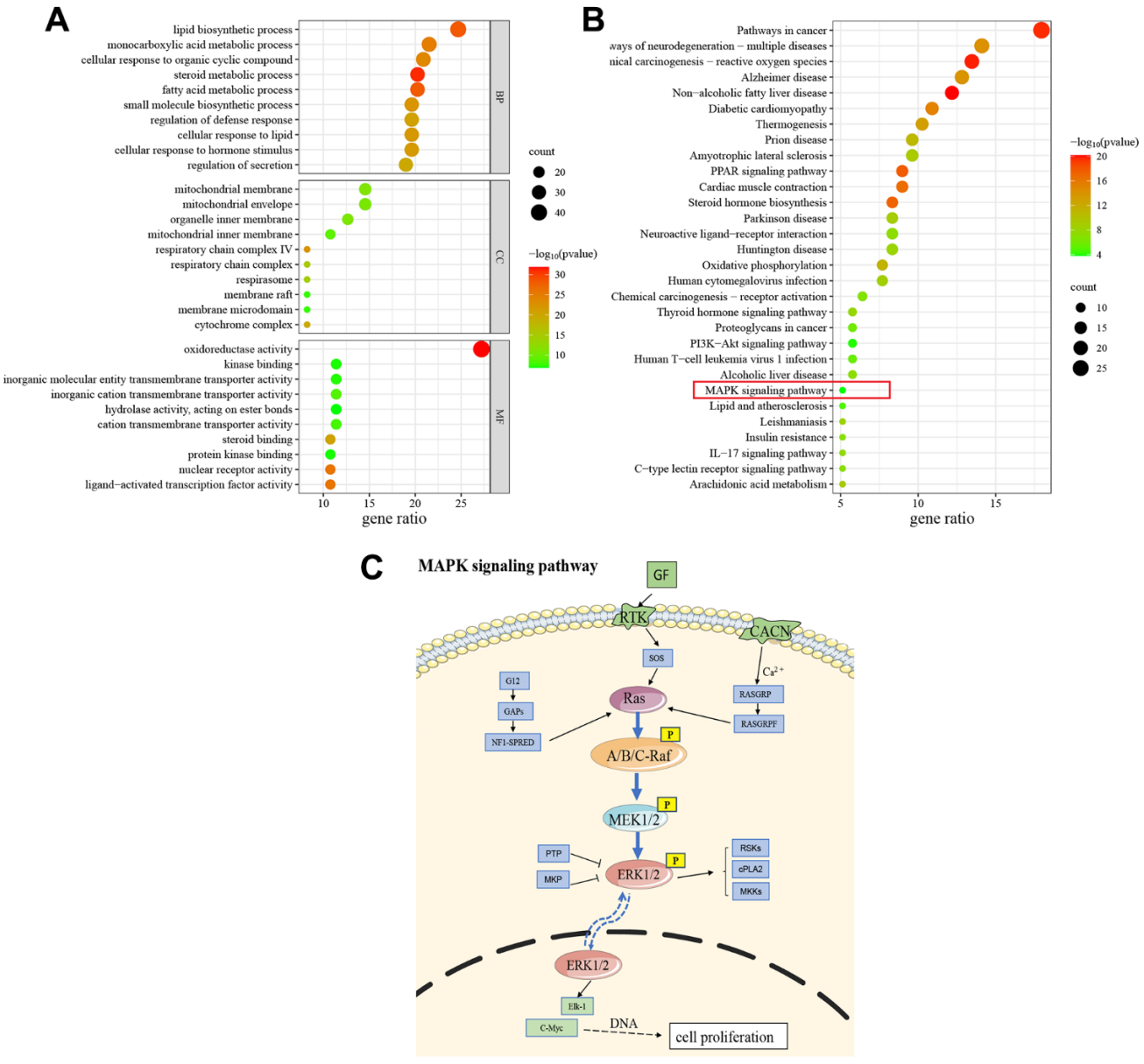

Figure 5. GO and KEGG enrichment analysis. (**A**) The results of GO enrichment analysis (Top 10). (**B**) The results of KEGG pathway enrichment analysis (Top 30). (**C**) Schematic drawing of the MAPK signaling pathway.

in the PPI network. Further analysis showed that MAPK3 was closely related to GC staging and prognosis in clinical correlation analysis. GO functional enrichment analysis identified common targets of GRA in the treatment of GC involved transmembrane transporters and nuclear receptor proteins, and KEGG enrichment results predicted that the MAPK signaling pathway may be a potential pathway for GRA in GC

A

Target	PDB ID	Energy(kcal/mol)	
		18α-GRA	18β-GRA
CTNNB1	5INV	-8.1	-7.9
AR	2YDV	-7.8	-8.3
IL 6	5FUC	-8.0	-8.2
MAPK3	2ZOQ	-7.0	-7.5
PTGS2	5F19	-8.5	-7.5
CYP19A1	3EQM	-7.5	-8.1
TNF	1D4V	-7.9	-8.3
PPARA	3ET1	-8.2	-7.6
PPARG	8DSZ	-5.2	-5.6
ESR1	6KN5	-7.8	-7.5

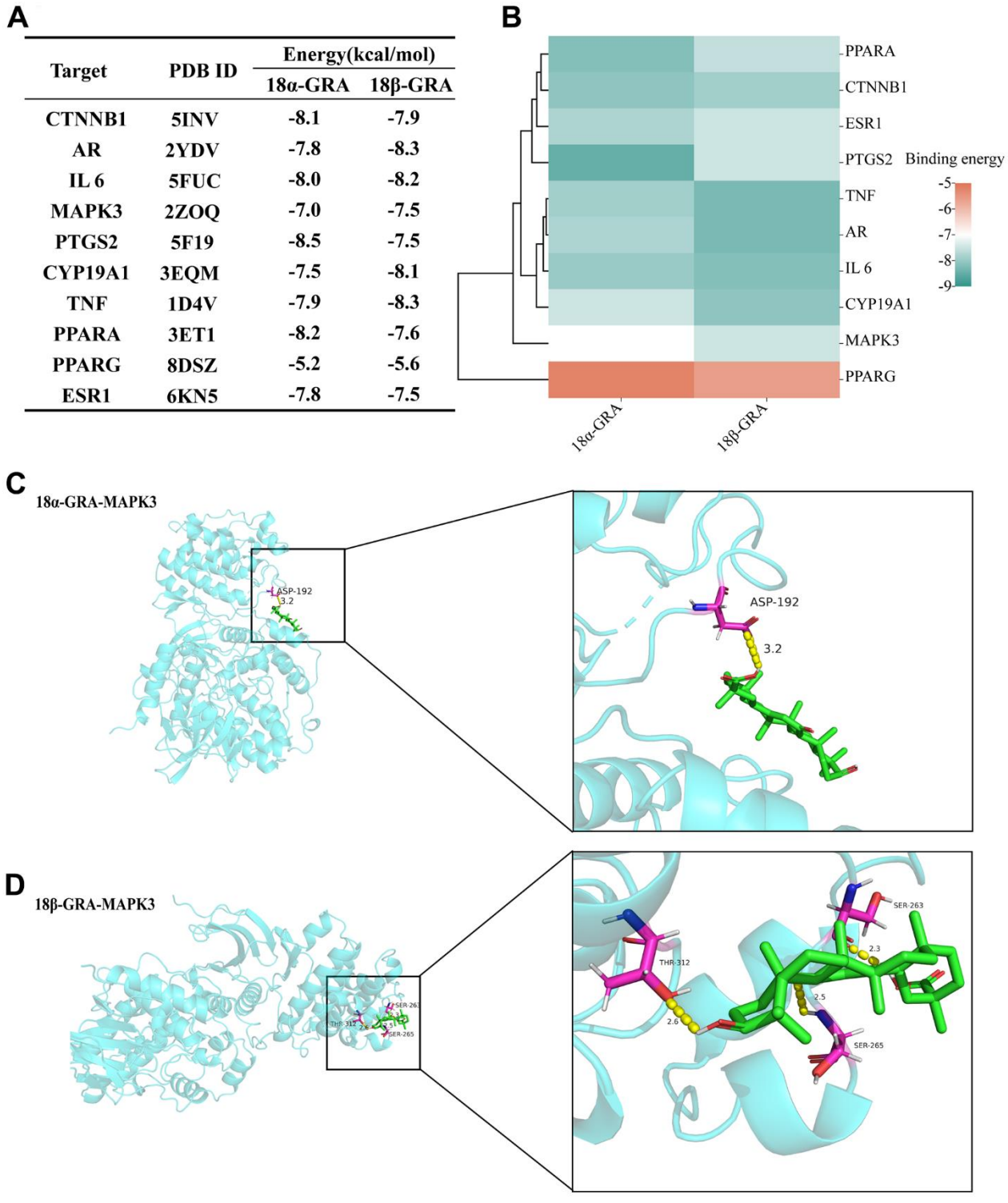

Figure 6. The results of molecular docking. (**A**) The results of molecular docking binding energy. (**B**) Heat map of molecular docking binding energy. (**C**) 18α-GRA and MAPK3 molecular docking visualization. (**D**) 18β-GRA and MAPK3 molecular docking visualization.

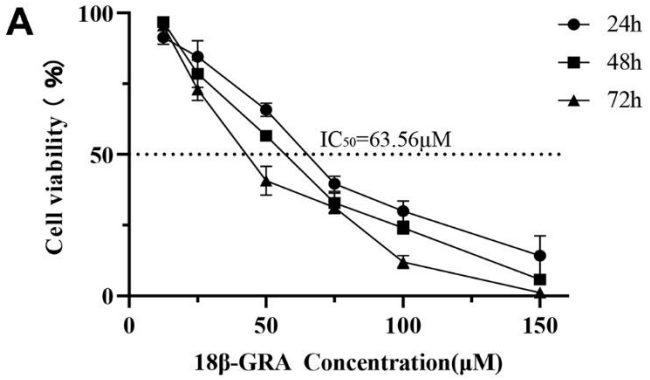

B

Cell line	IC50 (μM)		
	24h	48h	72h
AGS	63.56	53.65	42.93

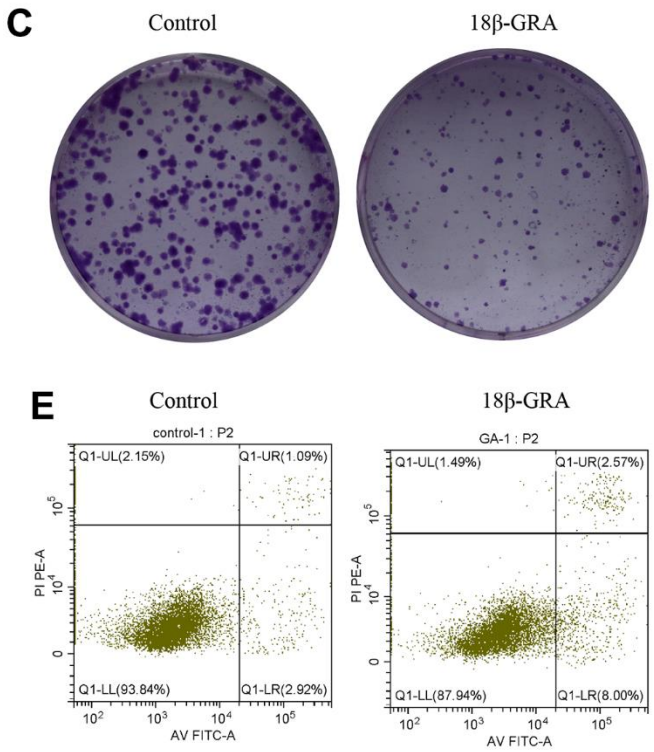

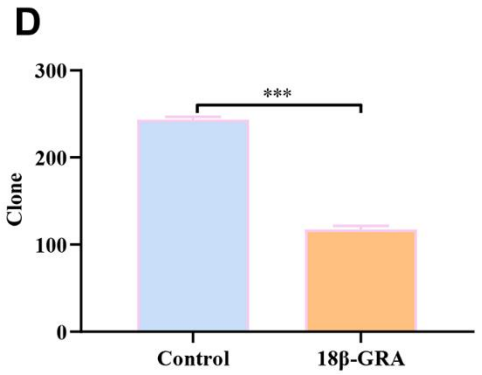

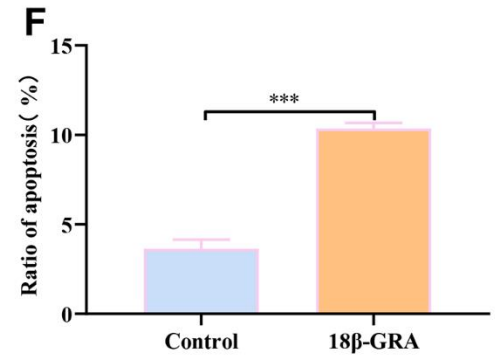

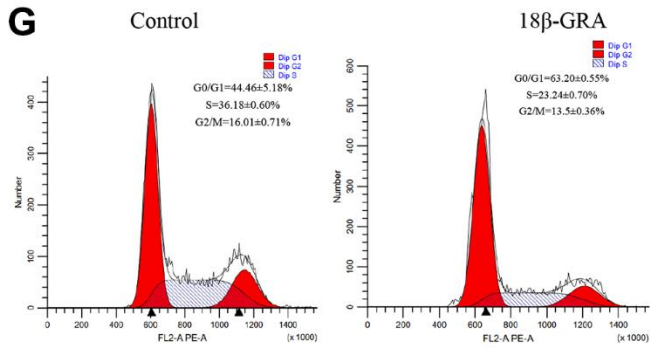

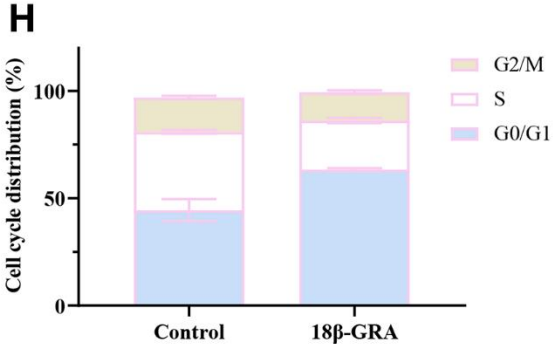

Figure 7. The effect of 18β-GRA on the phenotype of AGS cells. (**A**) The effect of 18β-GRA on AGS cells viability. (**B**) IC50 values of 18β-GRA interfered with AGS cells after 24 h, 48 h, and 72 h. (**C**, **D**) The results of colony formation and statistical chart. (**E**, **F**) The results of cell apoptosis and statistical chart. (**G**, **H**) The results of cell cycle and statistical chart. All the values are expressed as mean ± SD. Compared with the control group, ***$p < 0.001$.

therapy. In MAPK signaling pathway, KRAS is located on the cell membrane, and p-ERK1/2 can participate in signal transduction across the nuclear membrane. Furthermore, molecular docking predicted that GRA could strongly bind with MAPK3, one of the hub targets. To further verify the prediction, we conducted *in vitro* experiments to investigate the therapeutic potential of 18β-GRA on GC cells. The results showed that 18β-GRA could obviously inhibit GC cells proliferation, promote cell apoptosis, and arrest cell cycle.

It is well known that cell apoptosis plays an important role in various biological processes related to tumorigenesis [26]. The maintenance of cellular homeostasis relies on the balance between pro-apoptotic and anti-apoptotic signals [27], and the disruption of apoptotic regulatory pathways is a significant contributor to carcinogenesis [28]. Insufficient apoptosis resulting from a deficiency of appropriate pro-apoptotic signaling pathways or increase activity of anti-apoptotic factors can lead to continued proliferation of cancer cells. The processes of cell proliferation and

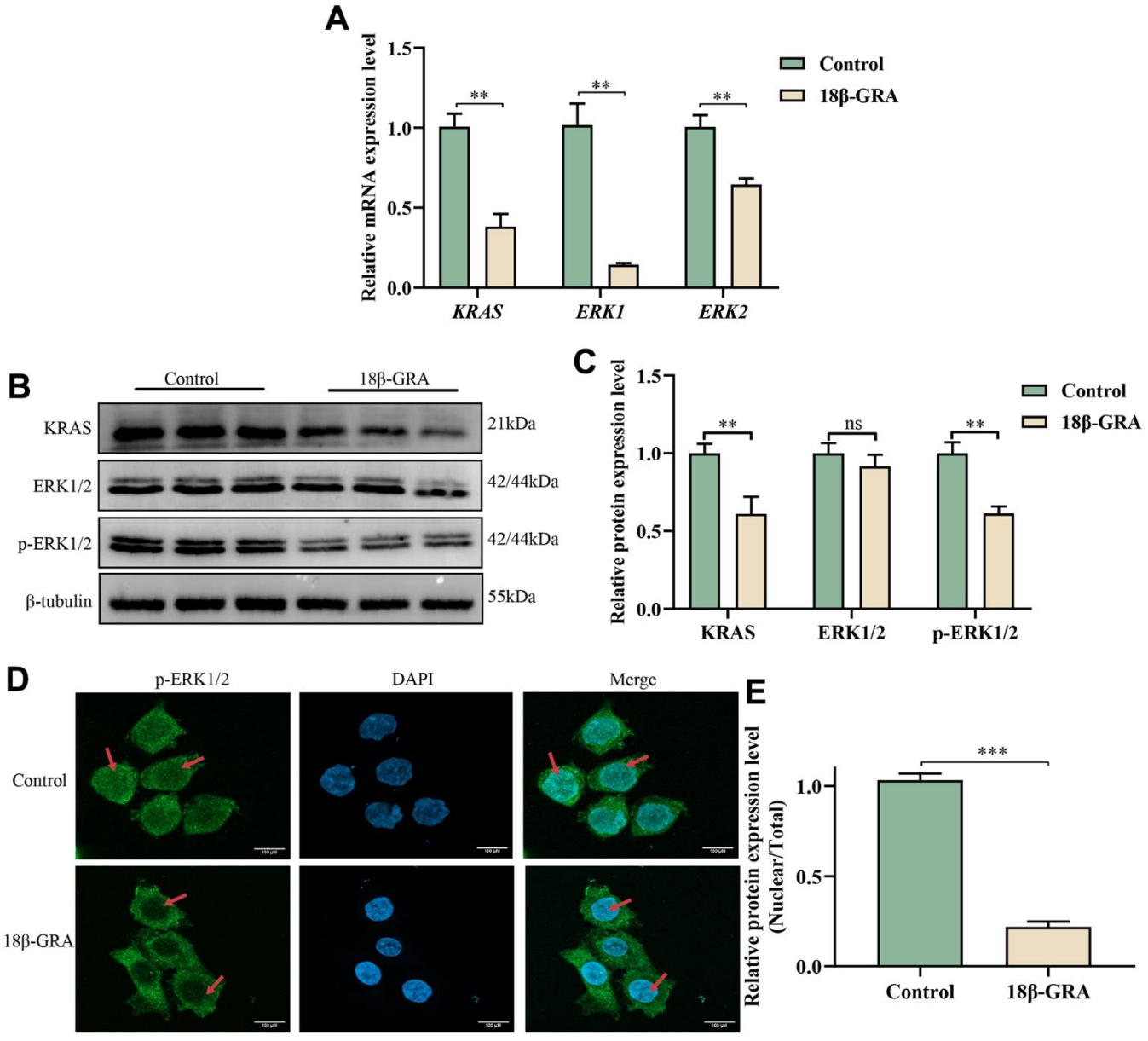

Figure 8. The effect of 18β-GRA on MAPK pathways in AGS cells. (**A**) qRT-PCR detection of *KRAS*, *ERK1*, and *ERK2* expression levels. (**B**) Western blotting analysis revealed the presence of KRAS, ERK1/2, p-ERK1/2 protein expression levels. (**C**) The results quantify protein levels of KRAS, ERK1/2 and p-ERK1/2 used Image J software. (**D**, **E**) The effects of 18β-GRA on nuclear transfer of p-ERK1/2 in AGS cells and statistical chart. All the values are expressed as mean ± SD. Compared with the control group, $^{**}p < 0.01$, $^{***}p < 0.001$.

cell cycle are inextricably linked [29]. Cell cycle progression involves the activation of various complexes that prevent cell from entering a new phase until the previous phase is successfully completed. Our results indicated that 18β-GRA promoted GC cells apoptosis and arrested cell cycle in the G0/G1 phase, thereby inhibiting their proliferation.

Tumor proliferation and growth relied on the activation and regulation of multiple signaling pathways. The MAPK signaling pathway is frequently activated in tumors and plays a crucial role in regulating cell growth, development, survival, differentiation, division and apoptosis [30]. ERK1 and ERK2, mitogen-activated protein kinases (MAPKs), are cytoplasmic kinases that are activated in response to various stimuli and are key elements of signaling from the cell surface to the interior of the cell [31]. They are also essential components in signal transduction from the surface to the interior of the cell. The MAPK signaling pathway plays an essential role in regulating cell growth, development and division. The pathway is composed of MAP3K, MAP2K, and MAPK, and follows a three-stage enzymatic reaction. Ras is a guanosine triphosphatase (GTPase) located in the cell membrane, which binds GTP proteins and activates the phosphorylation cascade to deliver cellular signals. Ras has three isoforms, namely K-Ras, H-Ras, and N-Ras, which are expressed widely [32]. The Ras-Raf-MEK-ERK signaling pathway consists of Ras acting as an upstream activator protein, MEK1/2 as a MAP2K, and ERK1/2 as a MAPK [33, 34]. Once activated, p-ERK1/2 can be transported to the nucleus, where it binds to transcription factors, ultimately affecting the expression of cell-related genes. Previous studies have shown that ERK1/2 is abundantly expressed in various human tumors, including GC, hepatocellular carcinoma, glioblastoma multiforme, breast cancer, and lung cancer [35–39]. In this study, the results of western blotting and qRT-PCR demonstrated that treatment with 18β-GRA in GC cells led to significant suppression of KRAS and p-ERK1/2 expression in the MAPK signaling pathway. Additionally, immunofluorescence experiments showed that 18β-GRA could affect the nuclear translocation of p-ERK1/2 and block its entry into the nucleus in GC cells. These findings provide evidence that 18β-GRA may have anti-GC properties by suppressing the expression of KRAS and p-ERK/2 in the MAPK signaling pathway, as well as blocking p-ERK1/2 from entering the nucleus and binding to related transcription factors in the nucleus.

In summary, this study showed that 18β-GRA can reduce GC cells clone formation ability, promote cell apoptosis and arrest cell cycle in the G0/G1 phase by suppressing the MAPK signaling pathway and thus inhibiting the proliferation of GC cells, which could provide a scientific basis for the related research of 18β-GRA in the treatment of GC. Nevertheless, our research is limited to *in vitro* cell experiments, and more experiments are needed to support our future research. Therefore, we will continue to explore the link between 18β-GRA and GC in the future with the following study. First, the therapeutic effect of 18β-GRA on GC is investigated by *in vivo* animal experiments. Second, to explore the effect of 18β-GRA in reducing chemotherapeutic drug sensitivity in combination with chemotherapy drugs. Third, the molecular mechanism of 18β-GRA in GC treatment through gene silencing, co-IP, EMSA, and other methods should be further investigated.

CONCLUSIONS

In this study, we investigated the molecular mechanism of 18β-GRA in the treatment of GC through network pharmacology and experimental verification. The results showed that 18β-GRA could inhibit the proliferation of GC cells by suppressing the MAPK signaling pathway, induce apoptosis, arrest cell cycle, and reduce colony forming ability. Our results confirm the reliability of network pharmacology analysis and provide a strong scientific basis for further research.

MATERIALS AND METHODS

Acquisition of GRA-related targets

We obtained the 2D or 3D structure of GRA by PubChem (https://pubchem.ncbi.nlm.nih.gov/). The TCMSP database (https://tcmsp-e.com/), the PharmMapper database (https://www.lilab-ecust.cn/pharmmapper/), the ETCM database (http://www.tcmip.cn/ETCM/index.php/Home/) and the SIB database (http://www.swisstargetprediction.ch/) were used to predict GRA targets. The search results were combined and deduplicated to obtain GRA-related targets.

Acquisition of GC-related targets

We searched the keywords “gastric cancer,” “stomach neoplasm,” “stomach cancer” and “gastric carcinoma,” from the GeneCards database (https://www.genecards.org/). Then, we combined and deduplicated the search results to obtain GC-related targets.

Protein-protein interaction (PPI) network analysis

We used the Venny 2.1.0 platform (https://bioinfogp.cnb.csic.es/tools/venny/index.html) to obtain the

common targets of GRA and GC, and make a Venn diagram. We entered the common targets into the STRING database (https://string-db.org/), selected Homo sapiens, and set the confidence range to "scoring value >0.7". Next, we downloaded the TSV file and uploaded it to the Cytoscape 3.8.2 to make the PPI network and filter hub targets based on degree ranking.

Clinical correlation analysis of hub targets

We downloaded GC patients' differentially expressed genes (DEGs) from the GEO database (https://www.ncbi.nlm.nih.gov/geo/), series: GES79973, then adjusted for $p < 0.05$ and $|\log 2 \text{ (fold change)}| > 1$. We used the GEPIA (http://GEPIA.cancer-pku.cn/) to obtain the expression levels of hub target gene in GC and normal tissues, and analyzed the differences and changes in expression level at different stages. We used the Kaplan-Meier plotter database (http://kmplot.com/analysis/) to analyze the hub target genes' influence on the prognosis of GC patients.

Enrichment analysis

We used the Metscape database (https://metascape.org/gp/index.html#/main/step1) to analyze Gene Ontology (GO) and Kyoto Encyclopedia of Genes and Genomes (KEGG) of common targets. Sort by the number of enrichments. We visualized the results as a bubble diagram.

Molecular docking

We obtained the protein structures of the hub targets from the PDB database (https://www.rcsb.org/) and used chem3D software to convert 2D structure to a 3D structure of GRA. We used the Auto Dock Tools to modify the protein [24], perform molecular docking of the receptor and the ligand, and evaluate the binding energy. We visualized the molecular docking results by Pymol.

Cell culture

Human GC cell line AGS cells (Cat. No. CL-0022, Procell, China) were cultured in DMEM/F12 medium which contain 10% fetal bovine serum (FBS, Cat. No. SH30256, Gibco, USA) in a humidity incubator with 5% CO_2 at 37° C.

Cell viability assay

We inoculated AGS cells in 96-well plates at 5×10^4 cells/ml and incubated for 24 h. Next, we added 18β-GRA (Cat. No. G10105-10G, Sigma, USA) at concentrations of 0-150 μM incubation was continued for 24 h, 48 h and 72 h. Then, we added 10 μl CCK-8 (Cat. No. KGRA317, KeyGEN, China) to each well and incubated for 2 h at 37° C. Finally, we detected optical density (OD) at 450 nm. All experimental groups repeated 4 wells.

Colony formation assay

We inoculated AGS cells in 6-well plates with 500 cells per well and incubated for 24 h, intervened with 18β-GRA and incubated for approximately 14 days. We used 4% paraformaldehyde to fixate the cells, crystal violet to stain, and distilled water to wash. Finally, the cell clones were photographed and statistical analysis based on clone sizes (Diameter > 1 mm). All experimental groups repeated 3 samples.

Cell apoptosis and cell cycle assay

We inoculated AGS cells in culture flask and incubated for 24 h, intervened with 18β-GRA. Next, we collected the cells and stained with an apoptosis detection kit (Cat. No. KGRA107, KeyGEN, China), then detected by flow cytometry. We collected the cells from each group, washed with PBS, and fixed overnight at 4° C with 70% ethanol. We stained the cells with a cell cycle kit (Cat. No. KGRA512, KeyGEN, China), and detected by flow cytometry. All experimental groups repeated 3 samples.

Quantitative real-time polymerase chain reaction (qRT-PCR)

We extracted the total RNA from AGS cells with Trizol (Cat. No. DP419, Tiagen Biochemical Technology, China). Subsequently, we synthesized cDNA based on the instructions of the PrimeScriptTM RT kit (Cat. No. RR047A, TaKaRa, Japan). We performed qRT-PCR with the SYBR Green kit (Cat. No. FP205, Tiagen Biochemical Technology, China). The expression levels of Kirsten rat sarcoma viral oncogene (*KRAS*), extracellular-regulated protein kinase 1 *(ERK1)*, and extracellular-regulated protein kinase 2 (*ERK2*) were quantified. The primer sequences are as follows: *KRAS*: forward: 5'-TGTGGACGAATATGATCCAACA-3', reverse: 5'- GCAAATACACAAAGAAAGCCCT-3'; *ERK1*: forward: 5'-ATGTCATCGGCATCCGAGAC-3', reverse: 5'- GGATCTGGTAGAGGAAGTAGCA -3'; *ERK2*: forward: 5'- TACACCAACCTCTCGT ACATCG -3', reverse: 5'- ATGTCTGAAGCGCAGT AAGATT -3'; *GAPDH*: forward: 5'- CACCCA CTCCTCCACCTTTGA -3', reverse: 5'- TCTCTCT TCCTCTTGTGCTCTCTTGC -3'. *GAPDH* was used as an internal reference gene. All experimental groups repeated 3 samples.

Western blotting

Western blotting detected changes in protein expression. 18β-GRA intervened in AGS cells for 24 h. We extracted the total protein by RIPA lysis buffer (Cat. No. PC102, Epizyme Biotech, China), assessed the protein content by the BCA method. Next, we separated the total protein by SDS-PAGE, transferred onto PVDF membranes (Cat. No. ISEQ00010, Millipore, USA), and sealed the membrane with 5% BSA for 1 h. After that, we incubated the membranes in the corresponding primary antibody overnight at 4° C. The corresponding primary antibodies included anti-KRAS (Cat. No. ab275876, Abcam, 1:1000), anti-ERK1/2 (Cat. No. 9102, CST, 1:2000), anti-p-ERK1/2 (Cat. No. 4370, CST, 1:2000), and anti-β-tubulin (Cat. No. 2146, CST, 1:5000). Moreover, we used TBST to wash the membranes 3 times and incubated them with anti-mouse/rabbit IgG antibodies (Cat. No. S0001 / S0002, Affinity, 1:5000) for 1 h. Finally, we detected the proteins by ECL and measured band intensities by ImageJ. All experimental groups repeated 3 samples.

Immunofluorescence

We treated AGS cells with 18β-GRA and fixated the cells with 4% paraformaldehyde. Afterwards, we used PBS to wash the cells three times, 0.5% Triton X-100 solution to treat for 15 min, and 5% BSA to seal for 1 h. After that, we used the primary antibody (p-ERK1/2, 1: 500) to incubate the cells overnight at 4° C. The next day, we used PBS to wash the cells again, added the fluorescent secondary antibody (Cat. No. 111-545-144, Jackson ImmunoResearch Inc, USA), and then incubated for 1 h. Subsequently, we stained the nucleus with DAPI for 5 min. We used confocal scanning microscopy (LSM 900, Zeiss, Germany) to take photos. All experimental groups repeated 3 samples.

Statistical analysis

All data were analyzed using GraphPad Prism 7 software and presented as the mean ± SD of at least three independent samples. Using t-tests analyzed the statistical differences, $p < 0.05$ indicated a significant difference.

Abbreviations

GRA: Glycyrrhetinic acid; GC: Gastric cancer; TCM: Traditional Chinese Medicine; TCMSP: Traditional Chinese Medicine Systems Pharmacology Database and Analysis Platform; PPI: protein-protein interaction; GO: Gene Ontology; KEGG: Kyoto Encyclopedia of Genes and Genomes; BP: biological processes; CC: cellular components; MF: molecular function; CCK-8: Cell Counting Kit-8 kit; KRAS: Kirsten rat sarcoma viral oncogene; ERK: extracellular-regulated protein kinase; qRT-PCR: Quantitative real-time polymerase chain reaction.

AUTHOR CONTRIBUTIONS

Xia Li carried out the majority of the experiments, analyzed the data, completed the figure production, and wrote the manuscript. Yuhua Du and Shicong Huang carried out a portion of the experiments, and participated in the production of the figures and the composition of the manuscript. Yi Yang and Doudou Lu carried out part of the experiments, and participated in the statistical analysis of the data. Junfei Zhang, Yan Chen and Lei Zhang performed the network pharmacology prediction. Ling Yuan and Yi Nan revised and improved the manuscript. All authors have read the manuscript and concur with the findings of the study.

ACKNOWLEDGMENTS

We sincerely thank the public databases for providing open-accessible and high-quality resources for researchers. We also sincerely thank and acknowledge Li-Qun Wang for statistical analysis assistance.

CONFLICTS OF INTEREST

All authors declare no financial or commercial conflict of interest to this study.

FUNDING

This research was funded by National Natural Science Foundation of China, No. 82260879; Ningxia Medical University Project, No. XZ2021005; Ningxia Natural Science Foundation, No. 2022AAC03144 and Ningxia Natural Science Foundation, No. 2022AAC02039.

REFERENCES

1. Smyth EC, Nilsson M, Grabsch HI, van Grieken NC, Lordick F. Gastric cancer. Lancet. 2020; 396:635–48. https://doi.org/10.1016/S0140-6736(20)31288-5 PMID:32861308

2. Pirzadeh M, Khalili N, Rezaei N. The interplay between aryl hydrocarbon receptor, H. pylori, tryptophan, and arginine in the pathogenesis of gastric cancer. Int Rev Immunol. 2022; 41:299–312. https://doi.org/10.1080/08830185.2020.1851371 PMID:33236682

3. Abbas M, Habib M, Naveed M, Karthik K, Dhama K, Shi M, Dingding C. The relevance of gastric cancer biomarkers in prognosis and pre- and post-

chemotherapy in clinical practice. Biomed Pharmacother. 2017; 95:1082–90. https://doi.org/10.1016/j.biopha.2017.09.032 PMID:28922727

4. Miller KD, Nogueira L, Mariotto AB, Rowland JH, Yabroff KR, Alfano CM, Jemal A, Kramer JL, Siegel RL. Cancer treatment and survivorship statistics, 2019. CA Cancer J Clin. 2019; 69:363–85. https://doi.org/10.3322/caac.21565 PMID:31184787

5. Liu H, Xu J, Yao Q, Zhang Z, Guo Q, Lin J. Rab7 Is Associated with Poor Prognosis of Gastric Cancer and Promotes Proliferation, Invasion, and Migration of Gastric Cancer Cells. Med Sci Monit. 2020; 26:e922217. https://doi.org/10.12659/MSM.922217 PMID:32591494

6. Seki H, Sawai S, Ohyama K, Mizutani M, Ohnishi T, Sudo H, Fukushima EO, Akashi T, Aoki T, Saito K, Muranaka T. Triterpene functional genomics in licorice for identification of CYP72A154 involved in the biosynthesis of glycyrrhizin. Plant Cell. 2011; 23:4112–23. https://doi.org/10.1105/tpc.110.082685 PMID:22128119

7. zhu Z, Tao W, Li J, Guo S, Qian D, Shang E, Su S, Duan JA. Rapid determination of flavonoids in licorice and comparison of three licorice species. J Sep Sci. 2016; 39:473–82. https://doi.org/10.1002/jssc.201500685 PMID:26608595

8. Shi X, Yu L, Zhang Y, Liu Z, Zhang H, Zhang Y, Liu P, Du P. Glycyrrhetinic acid alleviates hepatic inflammation injury in viral hepatitis disease via a HMGB1-TLR4 signaling pathway. Int Immunopharmacol. 2020; 84:106578. https://doi.org/10.1016/j.intimp.2020.106578 PMID:32416454

9. Liang S, Li M, Yu X, Jin H, Zhang Y, Zhang L, Zhou D, Xiao S. Synthesis and structure-activity relationship studies of water-soluble β-cyclodextrin-glycyrrhetinic acid conjugates as potential anti-influenza virus agents. Eur J Med Chem. 2019; 166:328–38. https://doi.org/10.1016/j.ejmech.2019.01.074 PMID:30731401

10. Hussain H, Ali I, Wang D, Hakkim FL, Westermann B, Ahmed I, Ashour AM, Khan A, Hussain A, Green IR, Shah STA. Glycyrrhetinic acid: a promising scaffold for the discovery of anticancer agents. Expert Opin Drug Discov. 2021; 16:1497–516. https://doi.org/10.1080/17460441.2021.1956901 PMID:34294017

11. Richard SA. Exploring the Pivotal Immunomodulatory and Anti-Inflammatory Potentials of Glycyrrhizic and Glycyrrhetinic Acids. Mediators Inflamm. 2021; 2021:6699560. https://doi.org/10.1155/2021/6699560 PMID:33505216

12. Chen J, Zhang ZQ, Song J, Liu QM, Wang C, Huang Z, Chu L, Liang HF, Zhang BX, Chen XP. 18β-Glycyrrhetinic-acid-mediated unfolded protein response induces autophagy and apoptosis in hepatocellular carcinoma. Sci Rep. 2018; 8:9365. https://doi.org/10.1038/s41598-018-27142-5 PMID:29921924

13. Yadav DK, Kalani K, Singh AK, Khan F, Srivastava SK, Pant AB. Design, synthesis and *in vitro* evaluation of 18β-glycyrrhetinic acid derivatives for anticancer activity against human breast cancer cell line MCF-7. Curr Med Chem. 2014; 21:1160–70. https://doi.org/10.2174/09298673113206660330 PMID:24180274

14. Luo YH, Wang C, Xu WT, Zhang Y, Zhang T, Xue H, Li YN, Fu ZR, Wang Y, Jin CH. 18β-Glycyrrhetinic Acid Has Anti-Cancer Effects via Inducing Apoptosis and G2/M Cell Cycle Arrest, and Inhibiting Migration of A549 Lung Cancer Cells. Onco Targets Ther. 2021; 14:5131–44. https://doi.org/10.2147/OTT.S322852 PMID:34712051

15. Li X, Liu Y, Wang N, Liu Y, Wang S, Wang H, Li A, Ren S. Synthesis and discovery of 18β-glycyrrhetinic acid derivatives inhibiting cancer stem cell properties in ovarian cancer cells. RSC Adv. 2019; 9:27294–304. https://doi.org/10.1039/c9ra04961d PMID:35529208

16. Cao D, Wu Y, Jia Z, Zhao D, Zhang Y, Zhou T, Wu M, Zhang H, Tsukamoto T, Oshima M, Jiang J, Cao X. 18β-glycyrrhetinic acid inhibited mitochondrial energy metabolism and gastric carcinogenesis through methylation-regulated TLR2 signaling pathway. Carcinogenesis. 2019; 40:234–45. https://doi.org/10.1093/carcin/bgy150 PMID:30364936

17. Li Y, Feng L, Song ZF, Li HB, Huai QY. Synthesis and Anticancer Activities of Glycyrrhetinic Acid Derivatives. Molecules. 2016; 21:199. https://doi.org/10.3390/molecules21020199 PMID:26861280

18. Cao D, Jia Z, You L, Wu Y, Hou Z, Suo Y, Zhang H, Wen S, Tsukamoto T, Oshima M, Jiang J, Cao X. 18β-glycyrrhetinic acid suppresses gastric cancer by activation of miR-149-3p-Wnt-1 signaling. Oncotarget. 2016; 7:71960–73. https://doi.org/10.18632/oncotarget.12443 PMID:27713126

19. Cai H, Chen X, Zhang J, Wang J. 18β-glycyrrhetinic acid inhibits migration and invasion of human gastric cancer

cells via the ROS/PKC-α/ERK pathway. J Nat Med. 2018; 72:252–9. https://doi.org/10.1007/s11418-017-1145-y PMID:29098529

20. Yuan L, Yang Y, Li X, Zhou X, Du YH, Liu WJ, Zhang L, Yu L, Ma TT, Li JX, Chen Y, Nan Y. 18β-glycyrrhetinic acid regulates mitochondrial ribosomal protein L35-associated apoptosis signaling pathways to inhibit proliferation of gastric carcinoma cells. World J Gastroenterol. 2022; 28:2437–56. https://doi.org/10.3748/wjg.v28.i22.2437 PMID:35979263

21. Yang J, Tian S, Zhao J, Zhang W. Exploring the mechanism of TCM formulae in the treatment of different types of coronary heart disease by network pharmacology and machining learning. Pharmacol Res. 2020; 159:105034. https://doi.org/10.1016/j.phrs.2020.105034 PMID:32565312

22. Zhang Z, Li B, Huang J, Huang S, He D, Peng W, Zhang S. A Network Pharmacology Analysis of the Active Components of the Traditional Chinese Medicine Zuojinwan in Patients with Gastric Cancer. Med Sci Monit. 2020; 26:e923327. https://doi.org/10.12659/MSM.923327 PMID:32866138

23. Li J, Ye M, Gao J, Zhang Y, Zhu Q, Liang W. Systematic Understanding of Mechanism of Yi-Qi-Huo-Xue Decoction Against Intracerebral Hemorrhagic Stroke Using a Network Pharmacology Approach. Med Sci Monit. 2020; 26:e921849. https://doi.org/10.12659/MSM.921849 PMID:32769962

24. Wang Y, Xu C, Xu B, Li L, Li W, Wang W, Wu M. Xiaoai Jiedu Recipe Inhibits Proliferation and Metastasis of Non-Small Cell Lung Cancer Cells by Blocking the P38 Mitogen-Activated Protein Kinase (MAPK) Pathway. Med Sci Monit. 2019; 25:7538–46. https://doi.org/10.12659/MSM.917115 PMID:31590176

25. Zhang Y, Li X, Xu X, Yang N. Mechanisms of Paeonia lactiflora in Treatment of Ulcerative Colitis: A Network Pharmacological Study. Med Sci Monit. 2019; 25:7574–80. https://doi.org/10.12659/MSM.917695 PMID:31594914

26. Song Y, Chang L, Wang X, Tan B, Li J, Zhang J, Zhang F, Zhao L, Liu G, Huo B. Regulatory Mechanism and Experimental Verification of Patchouli Alcohol on Gastric Cancer Cell Based on Network Pharmacology. Front Oncol. 2021; 11:711984. https://doi.org/10.3389/fonc.2021.711984 PMID:34540679

27. Elmore S. Apoptosis: a review of programmed cell death. Toxicol Pathol. 2007; 35:495–516. https://doi.org/10.1080/01926230701320337 PMID:17562483

28. Cotter TG. Apoptosis and cancer: the genesis of a research field. Nat Rev Cancer. 2009; 9:501–7. https://doi.org/10.1038/nrc2663 PMID:19550425

29. Eymin B, Gazzeri S. Role of cell cycle regulators in lung carcinogenesis. Cell Adh Migr. 2010; 4:114–23. https://doi.org/10.4161/cam.4.1.10977 PMID:20139697

30. Guo YJ, Pan WW, Liu SB, Shen ZF, Xu Y, Hu LL. ERK/MAPK signalling pathway and tumorigenesis. Exp Ther Med. 2020; 19:1997–2007. https://doi.org/10.3892/etm.2020.8454 PMID:32104259

31. Casar B, Sanz-Moreno V, Yazicioglu MN, Rodríguez J, Berciano MT, Lafarga M, Cobb MH, Crespo P. Mxi2 promotes stimulus-independent ERK nuclear translocation. EMBO J. 2007; 26:635–46. https://doi.org/10.1038/sj.emboj.7601523 PMID:17255949

32. Samatar AA, Poulikakos PI. Targeting RAS-ERK signalling in cancer: promises and challenges. Nat Rev Drug Discov. 2014; 13:928–42. https://doi.org/10.1038/nrd4281 PMID:25435214

33. Yang S, Liu G. Targeting the Ras/Raf/MEK/ERK pathway in hepatocellular carcinoma. Oncol Lett. 2017; 13:1041–7. https://doi.org/10.3892/ol.2017.5557 PMID:28454211

34. Mandal R, Becker S, Strebhardt K. Stamping out RAF and MEK1/2 to inhibit the ERK1/2 pathway: an emerging threat to anticancer therapy. Oncogene. 2016; 35:2547–61. https://doi.org/10.1038/onc.2015.329 PMID:26364606

35. Bang YJ, Kwon JH, Kang SH, Kim JW, Yang YC. Increased MAPK activity and MKP-1 overexpression in human gastric adenocarcinoma. Biochem Biophys Res Commun. 1998; 250:43–7. https://doi.org/10.1006/bbrc.1998.9256 PMID:9735328

36. Wang Z, Wang X, Rong Z, Dai L, Qin C, Wang S, Geng W. LncRNA LINC01134 Contributes to Radioresistance in Hepatocellular Carcinoma by Regulating DNA Damage Response via MAPK Signaling Pathway. Front Pharmacol. 2022; 12:791889. https://doi.org/10.3389/fphar.2021.791889 PMID:35173610

37. Moslah W, Aissaoui-Zid D, Aboudou S, Abdelkafi-Koubaa Z, Potier-Cartereau M, Lemettre A, ELBini-

Dhouib I, Marrakchi N, Gigmes D, Vandier C, Luis J, Mabrouk K, Srairi-Abid N. Strengthening Anti-Glioblastoma Effect by Multi-Branched Dendrimers Design of a Scorpion Venom Tetrapeptide. Molecules. 2022; 27:806. https://doi.org/10.3390/molecules27030806 PMID:35164071

38. Naranjo AI, González-Gómez MJ, Baladrón V, Laborda J, Nueda ML. Different Expression Levels of DLK2 Inhibit NOTCH Signaling and Inversely Modulate MDA-MB-231 Breast Cancer Tumor Growth *In Vivo*. Int J Mol Sci. 2022; 23:1554. https://doi.org/10.3390/ijms23031554 PMID:35163478

39. Yuan M, Zhai Y, Men Y, Zhao M, Sun X, Ma Z, Bao Y, Yang X, Sun S, Liu Y, Zhang W, Hui Z. Anlotinib Enhances the Antitumor Activity of High-Dose Irradiation Combined with Anti-PD-L1 by Potentiating the Tumor Immune Microenvironment in Murine Lung Cancer. Oxid Med Cell Longev. 2022; 2022:5479491. https://doi.org/10.1155/2022/5479491 PMID:35154567

SUPPLEMENTARY MATERIALS

Supplementary Table

Supplementary Table 1. The common target's degree value.

Number	Targets	Degree
1	TNF	53
2	IL6	52
3	CTNNB1	42
4	PPARG	39
5	PTGS2	38
6	ESR1	37
7	MAPK3	31
8	PPARA	28
9	AR	25
10	CYP19A1	25
11	NCOA1	24
12	PGR	23
13	NR3C1	22
14	NCOA2	21
15	CYP2E1	19
16	CYP17A1	18
17	MMP2	18
18	PTGS1	17
19	PRKCA	17
20	ESR2	16
21	ALOX5	16
22	MDM2	16
23	FABP4	15
24	FABP1	15
25	HSD3B1	15
26	NFKB1	14
27	SCD	14
28	PTPN11	14
29	AKR1C3	14
30	HSD11B1	14
31	PTGER4	14
32	CYP2C19	14
33	PTPN1	13
34	SRD5A1	13
35	PTGES	13
36	GJA1	12
37	PPARD	12
38	HMGCR	12
39	MMP3	11
40	NR1H4	11
41	NR1H3	11
42	PLA2G1B	11
43	NR3C2	11
44	TERT	10
45	NOS2	10
46	HSD17B2	10
47	HSD17B3	10
48	ALOX5AP	10

49	SHBG	10
50	FABP3	9
51	G6PD	9
52	CDC25B	9
53	MMP1	8
54	HSD11B2	8
55	GSTP1	8
56	ITGB2	8
57	NFKB2	8
58	TOP2A	8
59	CTNNA1	7
60	FABP5	7
61	FDFT1	7
62	ANXA1	7
63	FAAH	7
64	NR1I2	7
65	GLUL	6
66	NR1I3	6
67	PTPN6	6
68	ACP1	6
69	PTPN2	6
70	EPHA2	6
71	LTB4R	6
72	IDO1	6
73	CD81	6
74	BACE1	6
75	CDC25A	6
76	COX7A1	6
77	RORC	5
78	PTGER1	5
79	SLC6A3	5
80	SLC6A4	5
81	COX4I1	5
82	MT-CO1	4
83	JUP	4
84	NPPB	4
85	PTGDR2	4
86	PTGER2	4
87	PRKCH	4
88	BCHE	4
89	RORA	3
90	PTPRF	3
91	ESRRG	3
92	TRPA1	3
93	ITGAL	3
94	TOP1	3
95	FFAR1	2